SUPPORTING INFORMATION

Layered Nanostructured Ferroelectric Perovskite $Bi_5FeTi_3O_{15}$ for Visible-Light Photodegradation of Antibiotics

Reshalaiti Hailili,[a,b] Zhi-Qiang Wang,[c] Meiyue Xu,[d] Yuanhao Wang,[a] Xue-Qing Gong,[*c] Tao Xu,[*d] and Chuanyi Wang[*a]

[a]*Laboratory of Environmental Sciences and Technology, Xinjiang Technical Institute of Physics & Chemistry, Key Laboratory of Functional Materials and Devices for Special Environments, Chinese Academy of Sciences, Urumqi 830011, China*

[b]*The Graduate School of Chinese Academy of Science, Beijing 100049, China*

[c]*Research Institute of Industrial Catalysis, East China University of Science and Technology, Shanghai 200237, China.*

[d]*Department of Chemistry and Biochemistry, Northern Illinois University, DeKalb Illinois 60115, United States*

To whom correspondence should be addressed: E-mail: cywang@ms.xjb.ac.cn; xgong@ecust.edu.cn; txu@niu.edu

CONTENTS

Experimental Section

Synthesis of $Bi_5FeTi_3O_{15}$ Photocatalysts. All of the chemicals were analytically pure and used as received from commercial sources without further purification. $Bi_5FeTi_3O_{15}$ photocatalysts were synthesized through a hydrothermal process. In the typical synthesis, the 3.0 mmoL of $Ti(OC_4H_9)_4$, 5.0 mmoL $Bi(NO_3)_3{\cdot}5H_2O$, 1.0 mmoL of $Fe(NO_3)_3{\cdot}9H_2O$ and 30.0 mL water containing 5.0 mL HNO_3 was added to a vial containing in a Teflon-lined steel bomb. Upon the addition of water, the solution became white and opaque, indicating hydrolysis of $Bi(NO_3)_3{\cdot}5H_2O$, under vigorous stirring a concentrated aqueous solution of NaOH was added dropwise into the above solution until a yellow suspension was formed. After being stirred 40 min, the pH was moderated to 7.0−14.0 by using HCI or NaOH. To ensure full dispersion, the colloidal suspension was stirred for 5 h and transferred into a 50 mL Teflon−lined stainless steel. The autoclave was heated at 160 °C for 15 h at autogenous pressure, and the autoclave was cooled at a rate of 5 °C/min to 100 °C and then, further cooled to room−temperature at a rate of 3 °C/min. The obtained *samples* were separated by filtration, washed with deionized water and absolute alcohol several times, then dried at 60 °C overnight and collected for further characterizations.

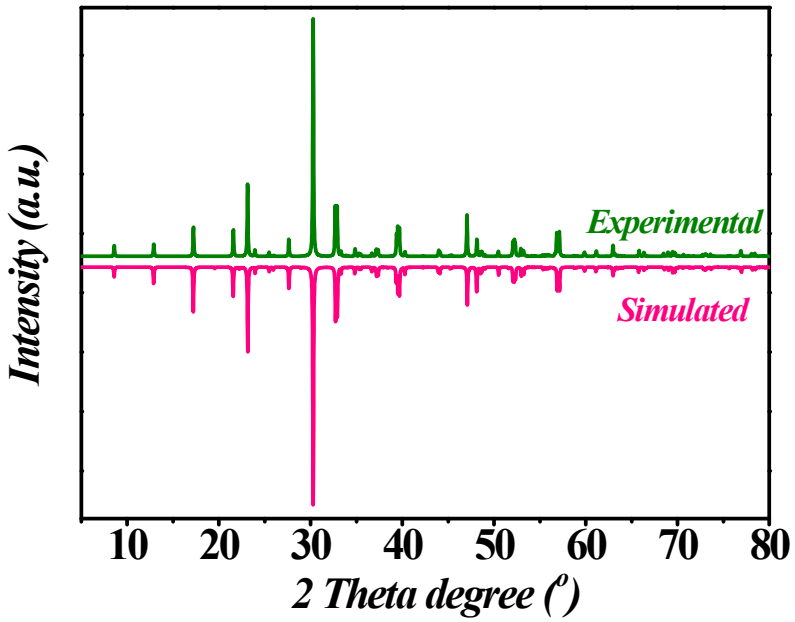

Figure S1. Simulated and experimental XRD patterns of $Bi_5FeTi_3O_{15}$ photocatalysts.

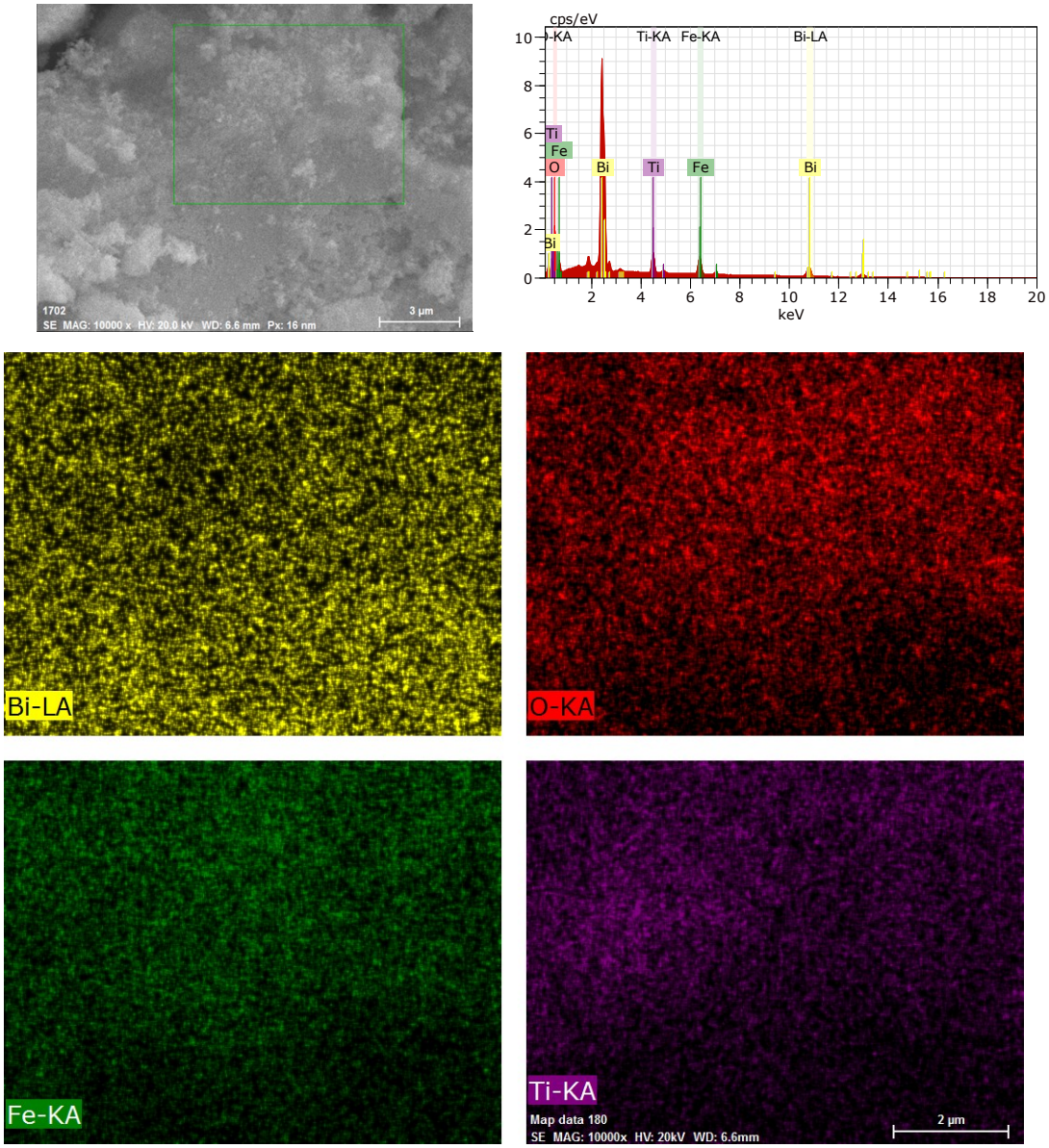

Figure S2. EDS elemental mapping of Bi, Ti, Fe and O in *sample* **1**

The *sample* **1** was consists of only from Bi, Fe, Ti and O, and all the elements are uniformly distributed on the surface of *sample* **1**.

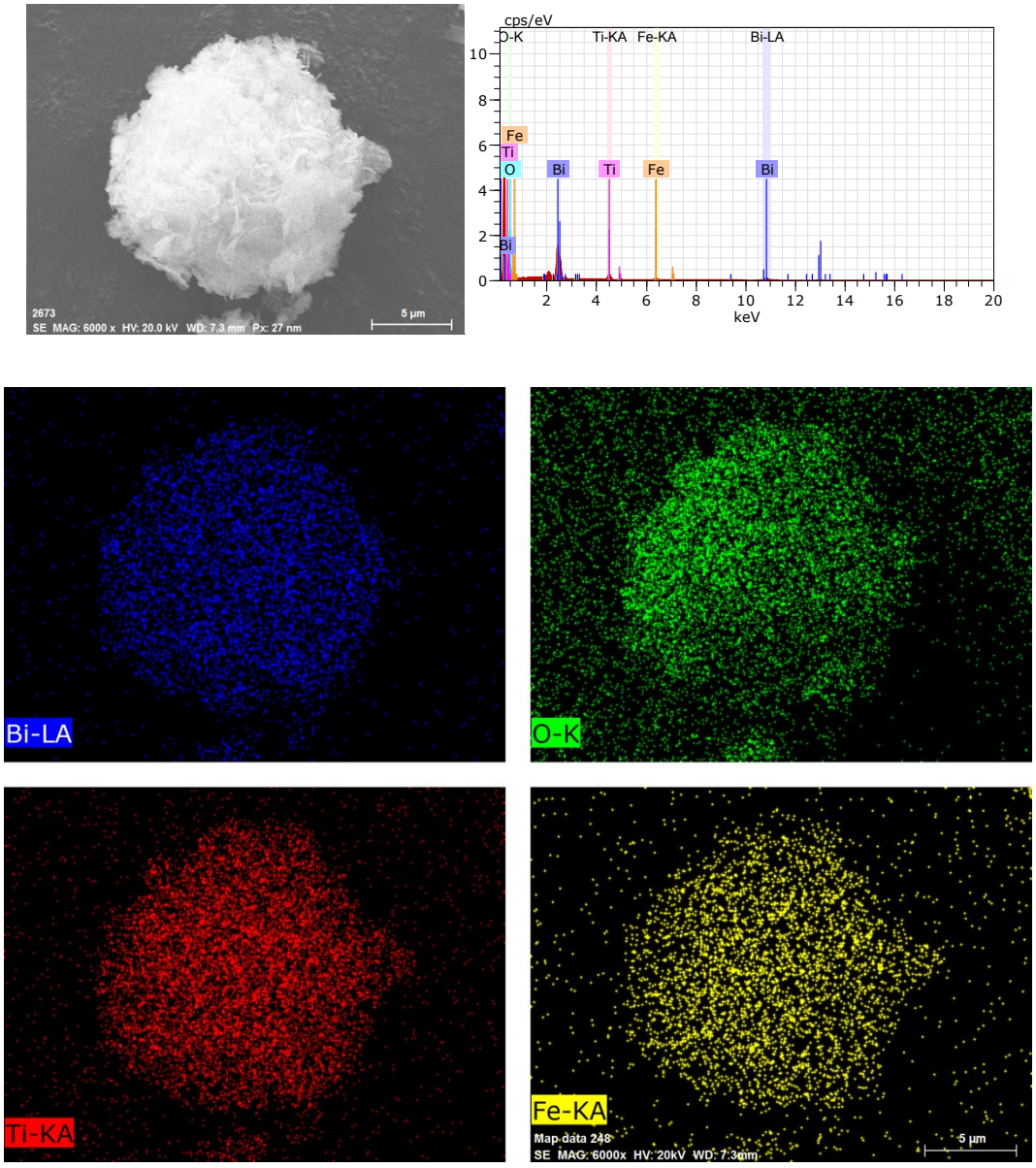

Figure S3. EDS elemental mapping of Bi, Ti, Fe and O in *sample* **6**

The *sample* **6** displays flower-like morphology and consists of Bi, Fe, Ti and O, and all the elements are uniformly distributed on the surface of *sample* **6**.

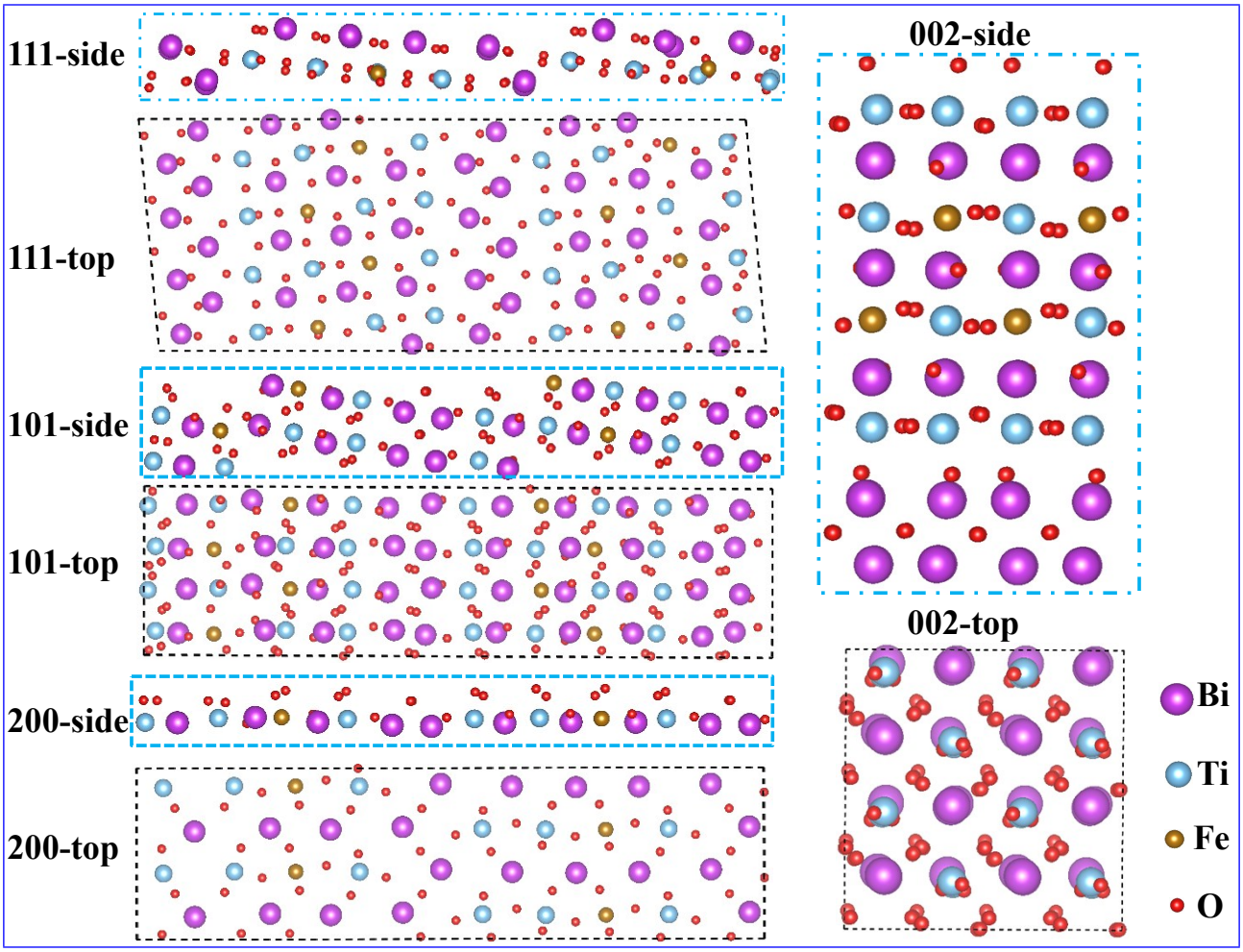

Figure S4. Surface atomic arrangements of $Bi_5FeTi_3O_{15}$ crystal.

Table S1. Comparison of different visible light active Fe-based photocatalysts for tetracycline removal.

Photocatalyst	Optimum conditions	Tetracycline removal at optimum condition (%)	Tetracycline removal at 60 min (%)	Ref.
$MgFe_2O_4$	0.1 g, 100 mL, 120 min	64.43	44	1
$NiFe_2O_4/Bi_2O_3$	0.1 g, 100 mL, 90 min	90.78	85	2
$NiFe_2O_4$	0.1 g, 100 mL, 90 min	47.43	33	2
$Fe_2O_3/MgFe_2O_4$	0.01 g, 100 mL, 120min	48.75	26	3
$Ag/Fe_3O_4/g{-}C_3N_4$	0.05 g, 100 mL, 90 min	88.52	62	4
$Fe_3O_4/g{-}C_3N_4$	0.08 g, 100 mL, 120 min	79.00	45	5
$CoFe_2O_4/Ag/Ag_3VO_4$	0.05 g, 100 mL, 8 min	61.48	NG	6
$Fe{-}SrTiO_3$	0.1 g, 100 mL, 80 min	71.61	68	7
$Ni_{(1-x)}Cu_{(x)}Fe_2O_4$	0.1 g, 100 mL, 360 min	78.17	12	8
$NiFe_2O_4$	0.1 g, 100 mL, 360 min	32.00	6	8
$SrTiO_3/Fe_2O_3$	0.1 g, 100 mL, 140 min	82.70	60	9
Fe_2O_3	0.1 g, 100 mL, 140 min	33.31	6	9
Ag/AgCl/(x)Fe(0)	0.01 g, 100 mL, 240 min	98.51	36	10
$Bi_5FeTi_3O_{15}$	0.04 g, 100 mL, 60 min	99.34	96.5 at **20** min	This work

*NG = Not given

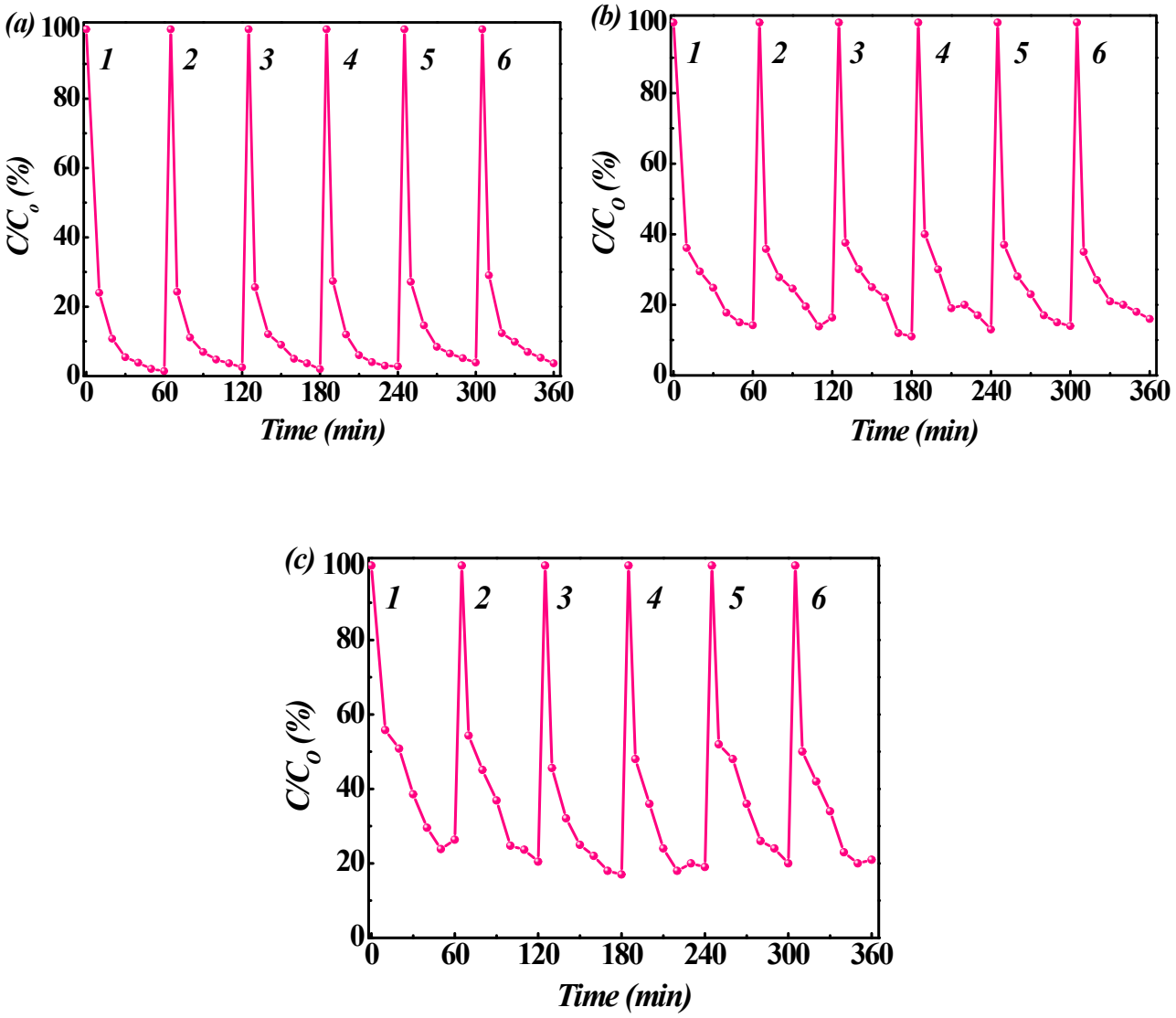

Figure S5. (a ~ c) Six run successive photodecomposition of tetracycline with *sample* **1**, *sample* **2** and *sample* **3** under visible light irradiation.

Figure **S**5 presents the tests of degradation percentage as a function of irradiation time in the presence of *sample* **1**−**3** over six cycles for tetracycline concentration changes detected at the maximum absorbance of 355 nm. It can be seen from stability test that as-obtained *samples* are still displayed high efficiency and stablility even after six cycles photocatalytic degradation (360 min) under visible light irradation.

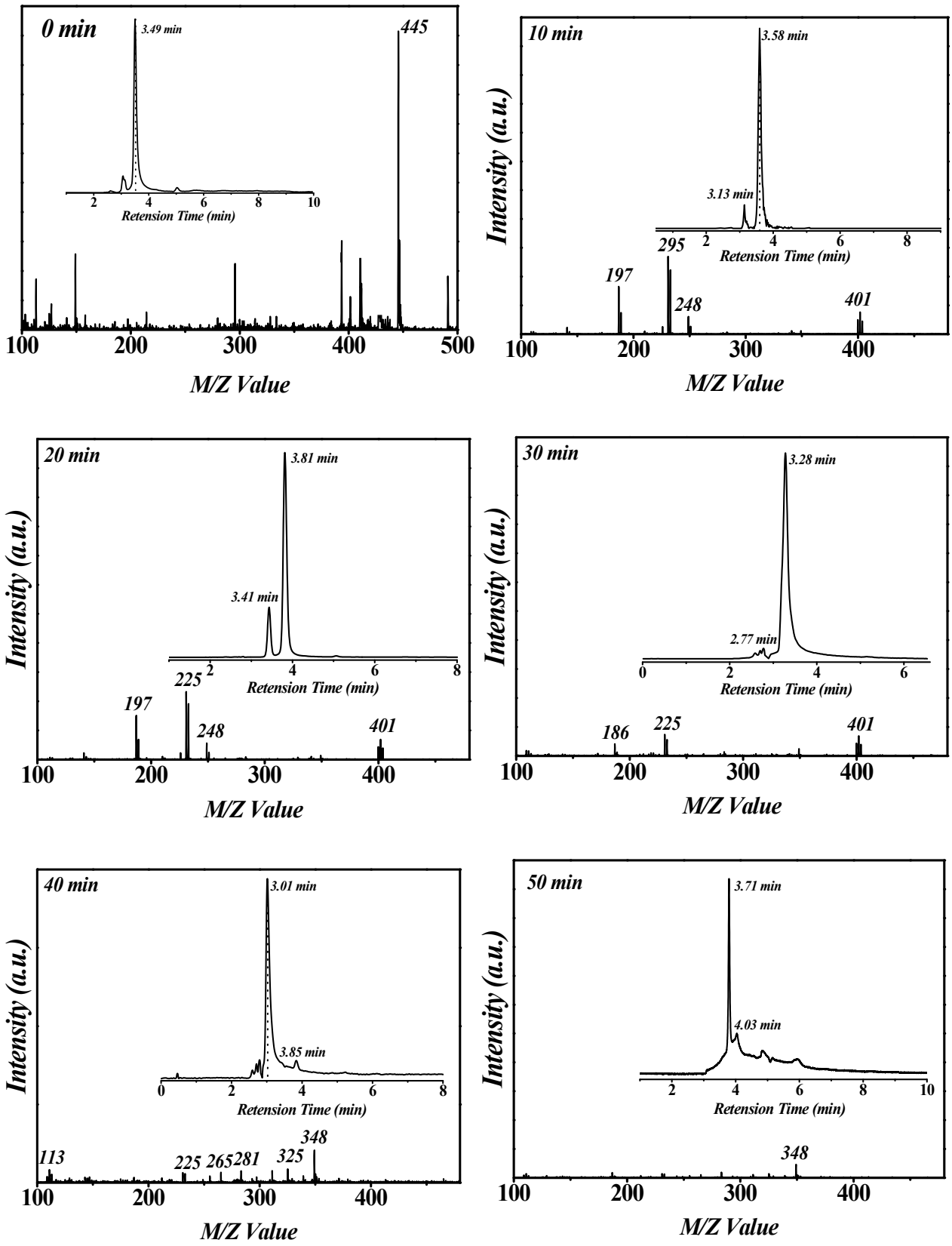

Figure S6. High-Performance Liquid Chromatography–Mass Spectrometry (LC-MS) analysis for all intermediates generated in tetracycline degradation in the presence of *sample* **6** under visible-light.

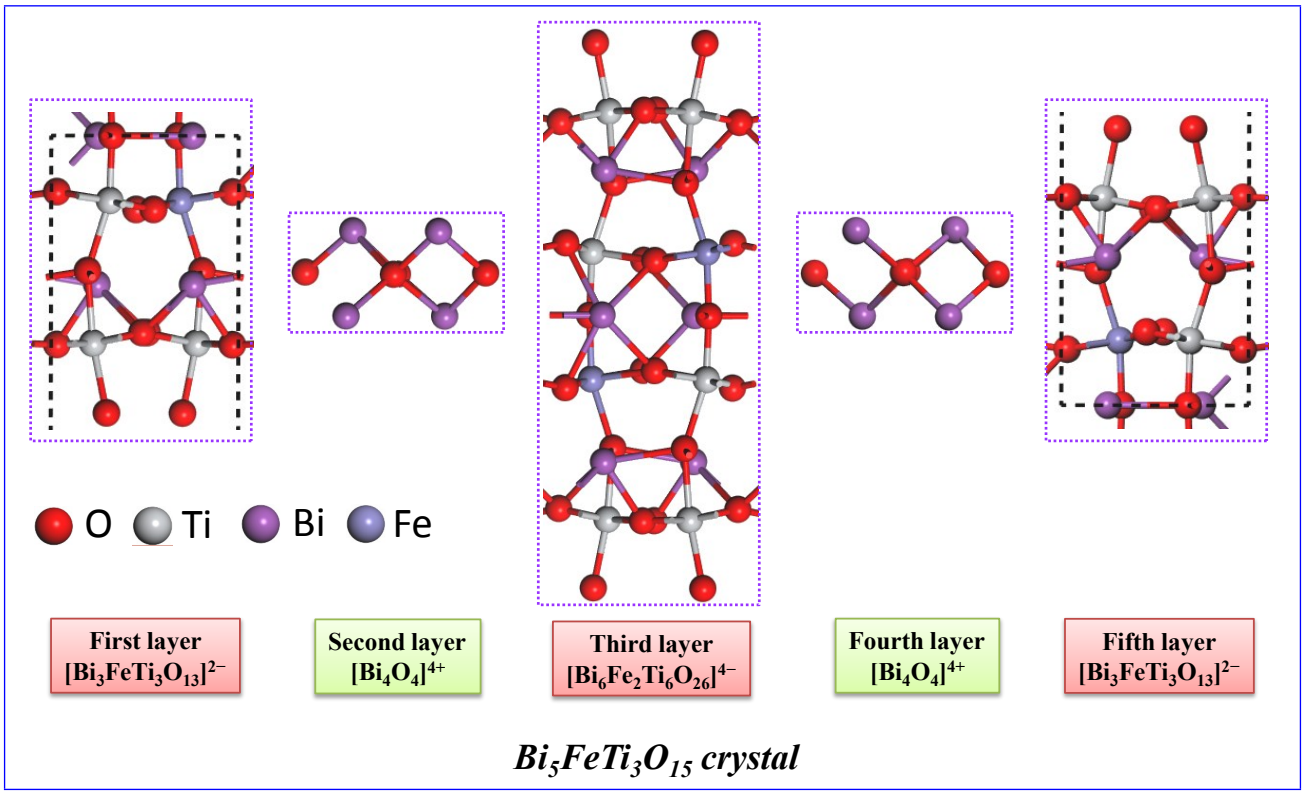

Figure S7. The selected different layers of $Bi_5FeTi_3O_{15}$ for calculation.

Table S2. The calculated DOS values within the 1.0 eV window above the CB minimum of different layers.

Layer	1	2	3	4	5
Integral	6.211	0.738	14.413	0.620	6.211
DOS (%)	22.03	2.62	51.12	2.20	22.03

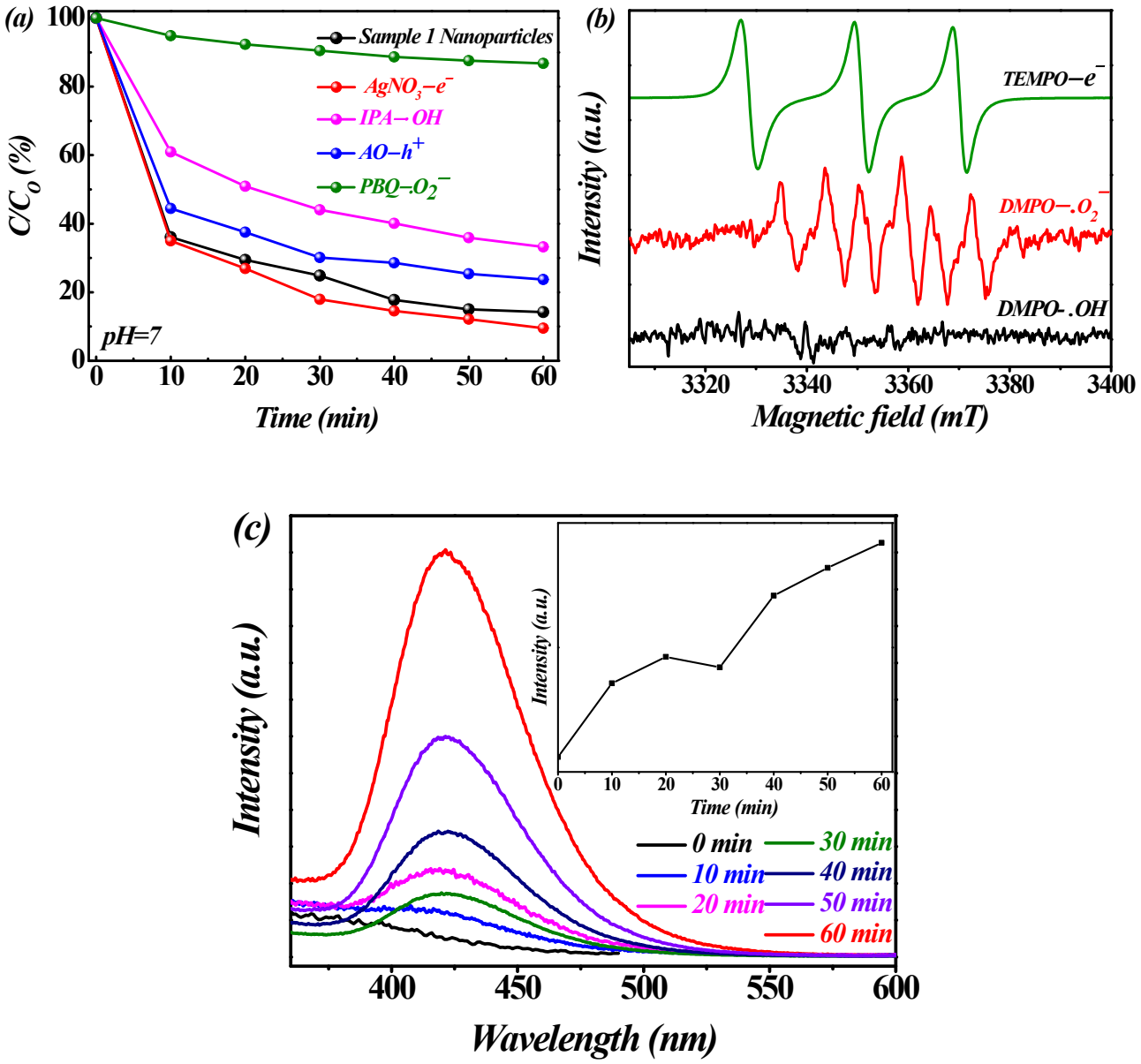

Figure S8. (a) Trapping studies of tetracycline degradation acticity over *sample* **1**; (b) ESR detection of superoxide, hydroxyl radicals using a DMPO spin−trapping agent. The methanol solution of DMPO was preirradiated in the presence of *sample* **1**; ESR detection of electrons with TEMPO spin−trapping agent (0.02 mM TEMPO) over *sample* **1**; (c) Hydroxyl radical ·OH detection photoluminescence (PL) spectra of *sample* **1** in 5.0 × 10^{-4} M basic solution of terephthalic acid under visible−light irradiation. Inset: the plot of the induced PL intensity (at 425.0 nm) *vs*. irradiation time.

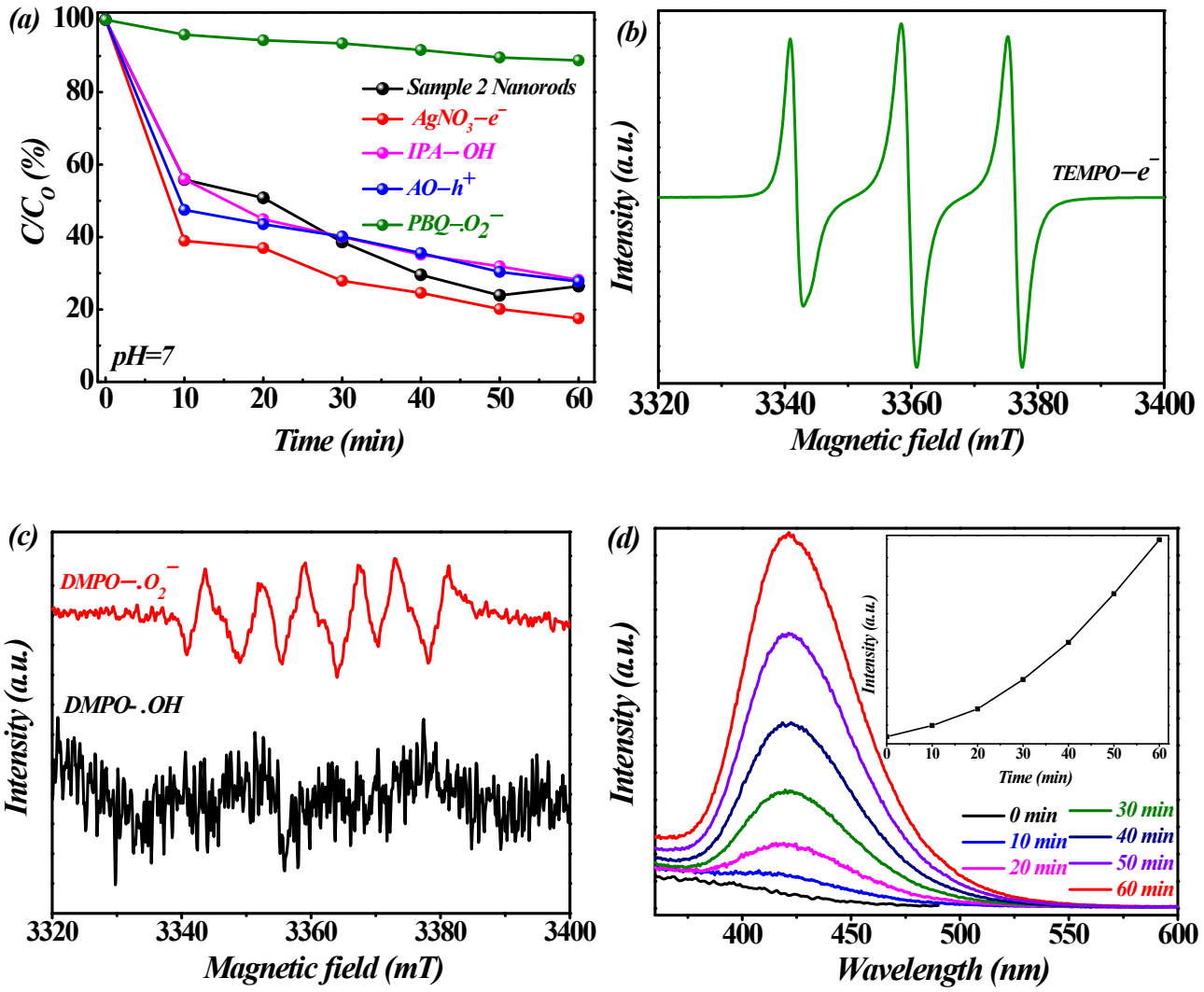

Figure S9. (a) Trapping studies of tetracycline degradation acticity over *sample* **2**; (b) ESR detection of electrons with TEMPO spin−trapping agent (0.02 mM TEMPO) over *sample* **2**; (c) ESR detection of superoxide, hydroxyl radicals using a DMPO spin−trapping agent. The methanol solution of DMPO was preirradiated in the presence of *sample* **2**; (d) Hydroxyl radical ·OH detection photoluminescence (PL) spectra of *sample* **2** in 5.0 × 10^{-4} M basic solution of terephthalic acid under visible−light irradiation. Inset: the plot of the induced PL intensity (at 425.0 nm) *vs*. irradiation time.

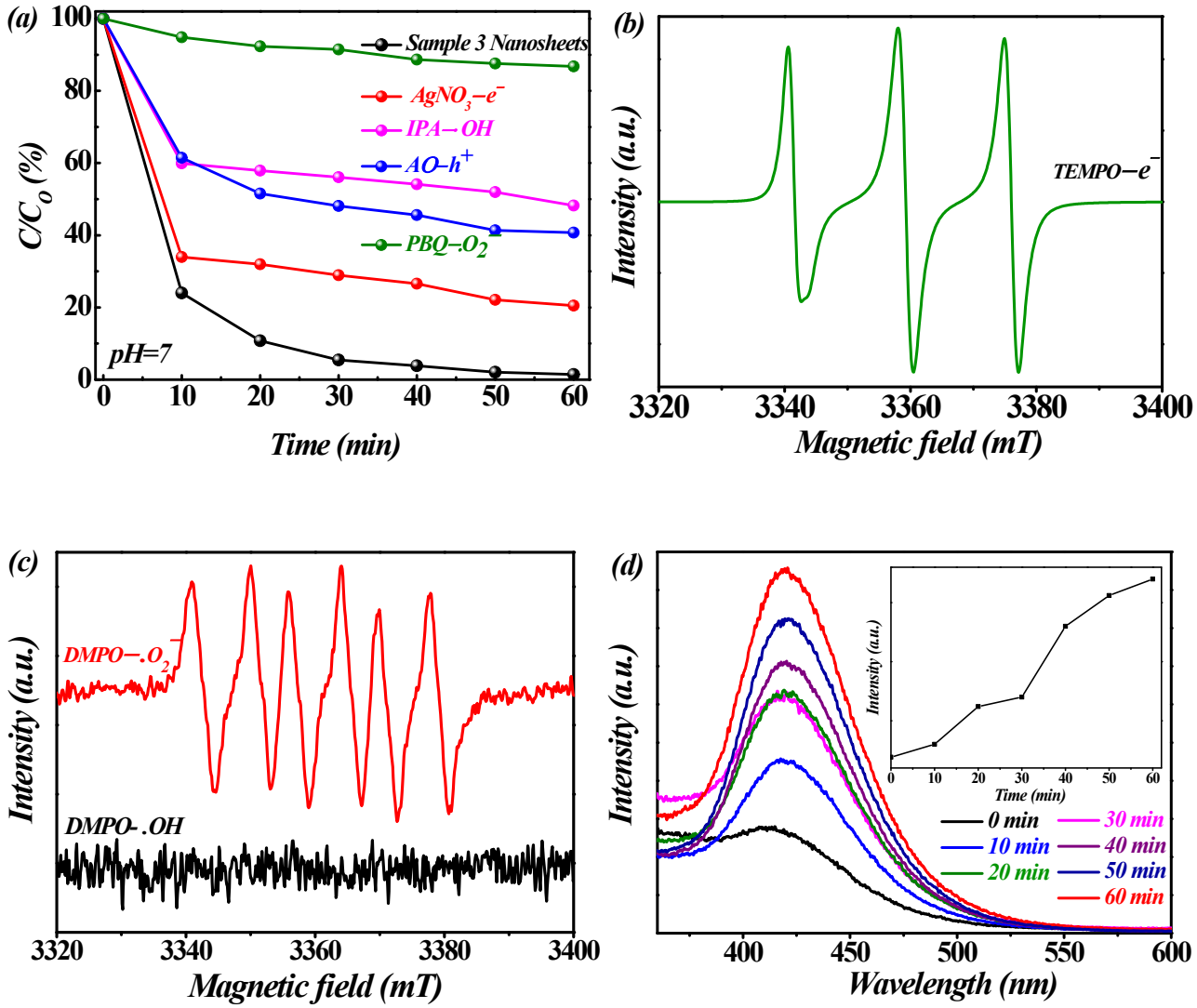

Figure S10. (a) Trapping studies of tetracycline degradation acticity over *sample* **3**; (b) ESR detection of electrons with TEMPO spin−trapping agent (0.02 mM TEMPO) over *sample* **3**; (c) ESR detection of superoxide, hydroxyl radicals using a DMPO spin−trapping agent. The methanol solution of DMPO was preirradiated in the presence of *sample* **3**; (d) Hydroxyl radical ·OH detection photoluminescence (PL) spectra of *sample* **3** in 5.0 × 10^{-4} M basic solution of terephthalic acid under visible−light irradiation. Inset: the plot of the induced PL intensity (at 425.0 nm) *vs*. irradiation time.

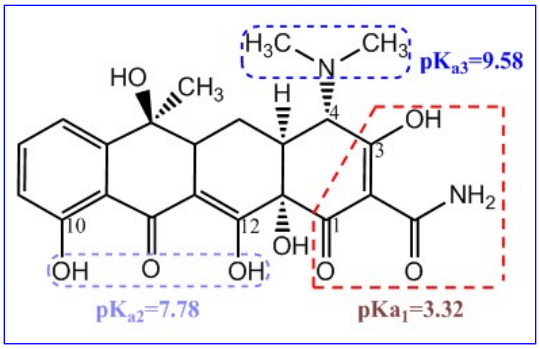

Figure S11. Structure and pK_a of tetracycline

Initial pH Influence for Tetracycline Degradation

To examine the influence of initial pH value on the stability and decomposition efficiency of tetracycline, the photocatalytic experiments were conducted within the pH range of 1.0 ~ 9.0 as shown in Figure **S**12. It can be seen that tetracycline shows unstable at higher pH media, on which tetracycline displays relatively higher degradation at alkaline media with the absence of photocatalyst. An initial influence of pH on tetracycline degradation was examined in the presence of *sample* **6**. Same decomposition trends were found with light irradiation over studied *sample* **6**.

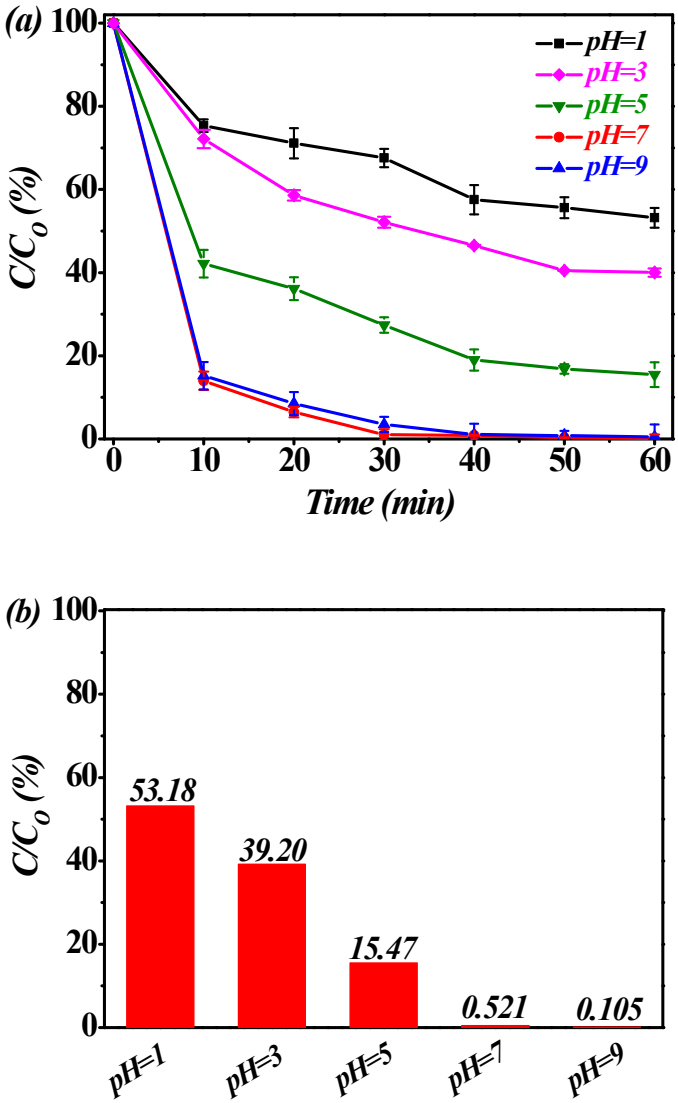

Figure S12. Initial pH influences to tetracycline degradation in the presence of *sample* **6**.

References

1. J. H. Jiang, W. Q. Fan, X. Zhang, H. Y. Bai, Y. Liu, S. Huang, B. D. Mao, S. L. Yuan, C. B. Liu, W. D. Shi, *New J. Chem.,* 2016, **40,** 538.
2. A. Ren, C. B. Liu, Y. Z. Hong, W. D. Shi, S. Lin, P. Li, *Chem. Eng. J.,* 2014, **258,** 301.
3. J. H. Jiang, K. L. Liu, W. Q. Fan, M. Li, Y. Liu, B. D. Mao, H. Y. Bai, H. Q. Shen, S. L. Yuan, W. D. Shi, *Mater. Lett.,* 2016, **176,** 1.
4. Z. Zhu, Z. Y. Lu, D. D. Wang, X. Tang, Y. S. Yan, W. D. Shi, Y. S. Wang, N. L. Gao, X. Yao, H. J. Dong, *Appl. Catal., B,* 2016, **182,** 115.
5. Z. Zhu, X. Tang, S. Kang, P. W. Huo, M. S. Song, W. D. Shi, Z. Y. Lu, Y. S. Yan, *J. Phys. Chem. C*, 2016, **120,** 27250.
6. L. Q. Jing, Y. G. Xu, S. Q. Huang, M. Xie, M. Q. He, H. Xua, H. M. Li, Q. Zhang, *Appl. Catal., B,* 2016, **199,** 11.
7. P. Li, C. B. Liu, G. L. Wu, Y. Heng, S. Lin, A. Ren, K. H. Lv, L. S. Xiao, W. D. Shi, *RSC Adv.,* 2014, **4,** 47615.
8. Y. Z. Hong, A. Ren, Y. H. Jiang, J. H. He, L. S. Xiao, W. D. Shi, *Ceram. Int.,* 2015, **41,** 1477.
9. C. B. Liu, G. L. Wu, J. B. Chen, K. Huang, W. D. Shi, *New J. Chem.,* 2016, **40,** 5198.
10. M. M. Liu, L.-A. Hou, B.-D. Xi, Q. Li, X. J. Hu, S. L. Yu, *Chem. Eng. J.,* 2016, **302,** 475.